



Paleoceanography and Paleoclimatology

RESEARCH ARTICLE

10.1029/2017PA003296

Key Points:

- Subarctic Pacific Ocean carbon dynamics is reconstructed using diatom carbon isotopes
- Net ocean-atmosphere CO₂ flux does not alter over the onset of major Northern Hemisphere Glaciation (circa 2.75–2.73 Ma)

Supporting Information:

- Supporting Information S1
- Table S1

Correspondence to:

G. E. A. Swann,
george.swann@nottingham.ac.uk

Citation:

Swann, G. E. A., Kendrick, C. P., Dickson, A. J., & Worne, S. (2018). Late Pliocene marine pCO₂ reconstructions from the subarctic Pacific Ocean. *Paleoceanography and Paleoclimatology*, 33. <https://doi.org/10.1029/2017PA003296>

Received 28 NOV 2017

Accepted 17 APR 2018

Accepted article online 27 APR 2018

Late Pliocene Marine pCO₂ Reconstructions From the Subarctic Pacific Ocean

George E. A. Swann¹ , Christopher P. Kendrick², Alexander J. Dickson³, and Savannah Worne¹

¹School of Geography, University of Nottingham, Nottingham, UK, ²NERC Isotope Geosciences Facility, British Geological Survey, Nottingham, UK, ³Department of Earth Sciences, Royal Holloway, University of London, Egham, UK

Abstract The development of large ice sheets across the Northern Hemisphere during the late Pliocene and the emergence of the glacial-interglacial cycles that punctuate the Quaternary mark a significant threshold in Earth's climate history. Although a number of different mechanisms have been proposed to initiate this cooling and the onset of major Northern Hemisphere glaciation, reductions in atmospheric concentrations of CO₂ likely played a key role. The emergence of a stratified (halocline) water column in the subarctic northwest Pacific Ocean at 2.73 Ma has often been interpreted as an event which would have limited oceanic ventilation of CO₂ to the atmosphere, thereby helping to cool the global climate system. Here diatom carbon isotopes ($\delta^{13}\text{C}_{\text{diatom}}$) are used to reconstruct changes in regional carbon dynamics through this interval. Results show that the development of a salinity stratification did not fundamentally alter the net oceanic/atmospheric flux of CO₂ in the subarctic northwest Pacific Ocean through the late Pliocene/early Quaternary. These results provide further insights into the long-term controls on global carbon cycling and the role of the subarctic Pacific Ocean in instigating global climatic changes.

1. Introduction

Understanding the processes associated with the progressive Late Pliocene glaciation of the Northern Hemisphere remains an essential objective for understanding the long-term functionality and temporal variability of the global climate system (Mudelsee & Raymo, 2005). Of particular note is the transition associated with the onset of major Northern Hemisphere Glaciation (oNHG) and its intensification (iNHG) from circa 2.75 to 2.73 Ma onward in Marine Isotope Stage (MIS) G6 when significant ice sheets developed across Greenland, Eurasia, and Northern America (Bailey et al., 2013; Kleiven et al., 2002; Maslin et al., 1996; Matthiessen et al., 2009; Raymo, 1994). Instrumental to this transition are Late Pliocene changes in solar insolation, tectonic uplift, water column stratification, and the opening/closure of oceanic gateways, all of which triggered oceanic/atmospheric feedbacks that initiated cooler conditions and the increased supply of moisture to high-latitude continental regions (Brierley & Fedorov, 2016; Driscoll & Haug, 1998; Haug & Tiedemann, 1998; Maslin et al., 1998; Ravelo et al., 2004; Ruddiman & Kutzbach, 1989; Sarnthein et al., 2009).

The extent to which variations in atmospheric pCO₂ (pCO_{2(atm)}) played a role in triggering both the oNHG and iNHG remains unconstrained. Ocean-atmospheric models have demonstrated that reductions in pCO_{2(atm)} were probably critical in both instigating and sustaining the development of large ice sheets through the oNHG (Bonelli et al., 2009; Frank et al., 2010; Lunt et al., 2008, 2010; Willeit et al., 2015), a view supported by most but not all pCO_{2(atm)} reconstructions (e.g., Badger et al., 2013; Martinez-Boti et al., 2015; Pagani et al., 2010; Seki et al., 2010; Stap et al., 2016; van de Wal et al., 2011; Willeit et al., 2015). With any significant change in pCO_{2(atm)} likely linked to oceanic atmosphere exchanges, a need exists to identify and evaluate possible marine sources/sinks of CO₂ through the late Pliocene.

1.1. Subarctic Northwest Pacific Ocean

The subarctic northwest Pacific Ocean (Figure 1) is one location that may have experienced significant changes in ocean atmospheric carbon dynamics through the late Pliocene and iNHG. Today the subarctic northwest Pacific Ocean acts as a net sink of atmospheric CO₂ due to a halocline driven stratification at a depth of ~150–200 m that minimizes deep water exposure at the ocean-atmosphere interface (Chierici et al., 2006; Honda et al., 2002; Tabata, 1975; Figure 1). Proxy data records from Ocean Drilling Program (ODP) Site 882 indicate that the halocline developed over the iNHG at 2.73 Ma with increases in surface freshwater transforming the mixed water column to a stratified system (Haug et al., 2005; Sigman et al., 2004; Swann, 2010;

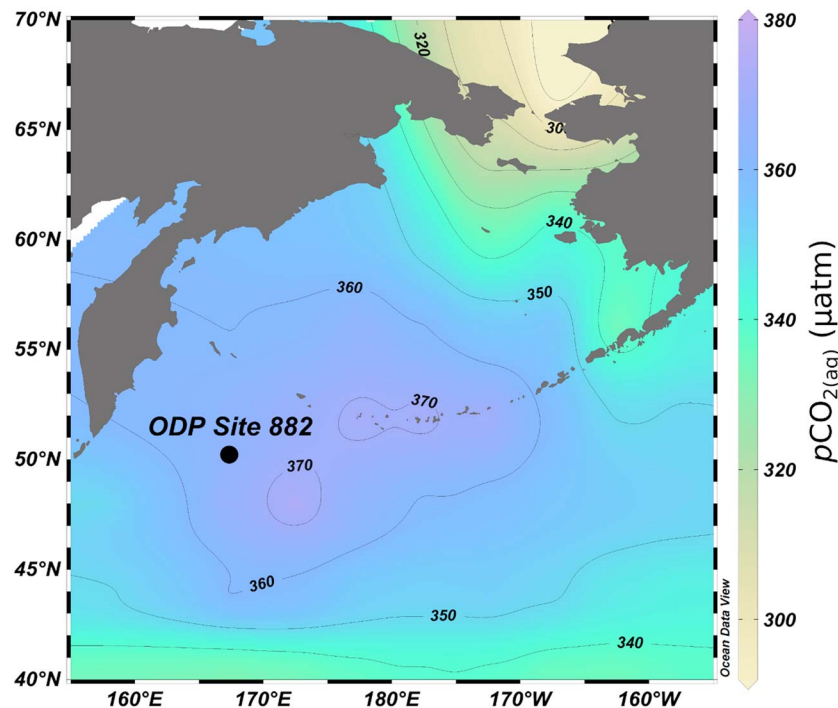


Figure 1. Location of ODP Site 882 (50°22'N, 167°36'E) in the northwest subarctic Pacific Ocean. Colors indicate annual modern gridded surface water $p\text{CO}_{2(\text{aq})}$ (Takahashi et al., 2016). Map created using Ocean Data View (<https://odv.awi.de>).

Swann et al., 2006). This development altered regional biogeochemical cycling (Bailey et al., 2011; Reynolds et al., 2008; Shimada et al., 2009; Studer et al., 2012; Swann et al., 2016) with a drop in opal mass accumulation rates (MAR) from $\sim 3 \text{ g}\cdot\text{cm}^{-2}\cdot\text{ka}^{-1}$ to $<1 \text{ g}\cdot\text{cm}^{-2}\cdot\text{ka}^{-1}$ at 2.73 Ma (Haug et al., 1999; Sigman et al., 2004).

These changes observed in the subarctic North Pacific Ocean may also have dramatically impacted ocean-atmosphere exchanges of CO_2 . With the deep North Pacific Ocean enriched in CO_2 relative to other ocean basins with dissolved inorganic carbon at $>2,300 \text{ }\mu\text{mol/kg}$ (Lauvset et al., 2016), a mixed water column prior to 2.73 Ma characterized by deep water upwelling may have ventilated CO_2 to the atmosphere, thereby helping to maintain the warm Pliocene climatic state (Haug et al., 1999). The emergence of a halocline from 2.73 Ma would have then minimized such exchanges, transforming the region to a net sink of atmospheric CO_2 similar to the modern day. This alteration in the direction of net ocean-atmosphere CO_2 exchange would have aided the iNHG and the global shift to colder climatic conditions (Haug et al., 1999). In an attempt to constrain the role of the subarctic Pacific in regulating the global climate system and $p\text{CO}_{2(\text{atm})}$ in the Piacenzian (3.60–2.58 Ma), diatom carbon isotopes ($\delta^{13}\text{C}_{\text{diatom}}$) are employed to reconstruct carbon dynamics in the subarctic northwest Pacific Ocean and assess their response to the expansion of ice sheets across the Northern Hemisphere over the iNHG and the transition to a stratified water column.

1.2. Reconstructing $p\text{CO}_2$ From $\delta^{13}\text{C}_{\text{diatom}}$

Hitherto, estimates of marine $p\text{CO}_2$ ($p\text{CO}_{2(\text{aq})}$) and $p\text{CO}_{2(\text{atm})}$ have been derived from the boron isotopes ($\delta^{11}\text{B}$) of foraminifera (Foster & Rae, 2016), the $\delta^{13}\text{C}$ composition of alkenones (Pagani, 2002), B/Ca measurements in foraminifera (Yu et al., 2007), fossil leaf stomata (Bai et al., 2015), and pedogenic carbonate (Montañez et al., 2016). Although each approach contains uncertainties and assumptions, the combination of approaches together with model simulations (Stap et al., 2016; van de Wal et al., 2011) are providing increasing consensus on the magnitude of past $p\text{CO}_{2(\text{atm})}$ and on the drivers, responses, and climate sensitivity of the Earth system.

Emerging work has promoted the use of $\delta^{13}\text{C}_{\text{diatom}}$ to reconstruct $p\text{CO}_{2(\text{atm})}$ (Heureux & Rickaby, 2015; Mejía et al., 2017; Stoll et al., 2017). The intrinsic organic carbon matter in diatoms frustules is comprised of proteins and polyamines that forms a key template for diatom biomineralization (Hecky et al., 1973; Kröger et al., 1999,

2000; Swift & Wheeler, 1992; Sumper & Kröger, 2004). During the photosynthetic production of this organic matter, diatoms preferentially fractionate ^{12}C over ^{13}C with the isotopic composition of $\delta^{13}\text{C}_{\text{diatom}}$:

$$\delta^{13}\text{C}_{\text{diatom}} = \delta^{13}\text{C}_{\text{DIC}} - \varepsilon_p - (\varepsilon_f - \varepsilon_p) \frac{C_i}{C_e} \quad (1)$$

where $\delta^{13}\text{C}_{\text{DIC}}$ is the isotopic value of the dissolved inorganic carbon (DIC) substrate, ε_p is the isotopic fractionation for the diffusion of carbon into the cell, ε_f is the isotopic fractionation associated with carbon capture by the photosynthetic enzyme RuBisCO having been constrained at +25‰ by Bidigare et al. (1997) and where C_i and C_e are the intracellular and extracellular concentrations of CO_2 in the water column ($\text{CO}_{2(\text{aq})}$; Laws et al., 1995; Rau et al., 1996, 1997). Accordingly, $\delta^{13}\text{C}_{\text{diatom}}$ can be linked to factors including changes in (1) $\delta^{13}\text{C}_{\text{DIC}}$ arising from changes in ocean circulation and the production/dissolution of carbonate producers, (2) photic zone $p\text{CO}_{2(\text{aq})}$ with increases (decreases) triggering a corresponding decrease (increase) in $\delta^{13}\text{C}_{\text{diatom}}$ through modification of $C_i:C_e$, and (3) photosynthetic carbon demand with increases causing a ^{12}C depletion in ambient seawater and so increasing $\delta^{13}\text{C}_{\text{diatom}}$. Attempts to reconstruct $p\text{CO}_{2(\text{aq})}$ have mainly focused on ε_p (the fractionation between diatom bound carbon and $\text{CO}_{2(\text{aq})}$):

$$\varepsilon_p = \left[\frac{\delta^{13}\text{CO}_{2(\text{aq})} + 1000}{\delta^{13}\text{C}_{\text{diatom}} + 1000} - 1 \right] \cdot 10^3 \quad (2)$$

In turn, $\delta^{13}\text{CO}_{2(\text{aq})}$ can be calculated from the $\delta^{13}\text{C}$ of planktonic carbonate ($\delta^{13}\text{C}_{\text{carbonate}}$), such as a planktonic foraminifera, building on the temperature-dependent fractionation between HCO_3^- and $\text{CO}_{2(\text{aq})}$ at a given sea surface temperature (T ; Mook et al., 1974; Romanek et al., 1992):

$$\delta^{13}\text{CO}_{2(\text{aq})} = \left(\frac{\varepsilon_{\text{CO}_{2(\text{aq})}-\text{CO}_{2(\text{g})}}}{1000} + 1 \right) \cdot (\delta^{13}\text{CO}_{2(\text{g})} + 1,000) - 1,000 \quad (3)$$

$$\varepsilon_{\text{CO}_{2(\text{aq})}-\text{CO}_{2(\text{g})}} = \frac{-373}{T + 273.15} + 0.19 \quad (4)$$

$$\delta^{13}\text{CO}_{2(\text{g})} = \frac{\delta^{13}\text{C}_{\text{carbonate}} + 1000}{\varepsilon_{\text{calcite}-\text{CO}_{2(\text{aq})}}/1000 + 1} \quad (5)$$

$$\varepsilon_{\text{calcite}-\text{CO}_{2(\text{g})}} = 11.98 - 0.12T \quad (6)$$

By targeting marine sediments in which both diatoms and planktonic foraminifera are preserved in the sediment record, $\delta^{13}\text{C}_{\text{diatom}}$ and $\delta^{13}\text{C}_{\text{foram}}$ can be combined to obtain absolute values of $\text{CO}_{2(\text{aq})}$ in the ambient photic zone waters:

$$\text{CO}_{2(\text{aq})} = \frac{b}{\varepsilon_f - \varepsilon_p} \quad (7)$$

where ε_f is the isotopic fractionation during carbon fixation which has been constrained as 25‰ (Bidigare et al., 1997) and b is the combination of physiological factors relating to cell size and growth rate. From this relationship, $p\text{CO}_{2(\text{aq})}$ can be calculated using Henry's law via the solubility coefficient K_H (Weiss, 1970, 1974):

$$p\text{CO}_{2(\text{aq})} = \frac{\text{CO}_{2(\text{aq})}}{K_H} \quad (8)$$

from which differences between $p\text{CO}_{2(\text{aq})}$ and $p\text{CO}_{2(\text{atm})}$ can be calculated as

$$\Delta p\text{CO}_2 = p\text{CO}_{2(\text{aq})} - p\text{CO}_{2(\text{atm})} \quad (9)$$

In instances where equilibrium exists between the surface ocean and the atmosphere, $\Delta p\text{CO}_2$ should be zero. Where the two system are not in equilibrium, $\Delta p\text{CO}_2$ provides insights into the net exchange between the two systems with positive (negative) values of $\Delta p\text{CO}_2$ indicating the marine system acts a source (sink) of atmospheric CO_2 .

An advantage in using $\delta^{13}\text{C}_{\text{diatom}}$ to reconstruct $p\text{CO}_{2(\text{aq})}$ is the widespread abundance of well-preserved diatoms in sediments across the globe, particularly in polar regions where carbonates are not readily preserved. However, while clear evidence exists that diatom carbon fixation is linked to $\text{CO}_{2(\text{aq})}$ (Popp et al., 1998; Rosenthal et al., 2000), reconstructions of $p\text{CO}_{2(\text{aq})}$ require robust estimates of b that accounts for physiological fractionation effects in $\delta^{13}\text{C}_{\text{diatom}}$ including those related to growth rate and cell size

(Bidigare et al., 1997; Laws et al., 1995, 2002). For example, alkenone $\delta^{13}\text{C}$ reconstructions of $p\text{CO}_{2(\text{aq})}$ rely on the strong relationship between b and PO_4^{3-} concentrations in the modern water column (Bidigare et al., 1997; Pagani et al., 2005). Recent work has demonstrated a strong link between b in diatoms and measures of productivity/growth rate such as opal concentrations, thereby allowing reconstructions of $p\text{CO}_{2(\text{aq})}$ from $\delta^{13}\text{C}_{\text{diatom}}$ (Heureux & Rickaby, 2015; Stoll et al., 2017).

2. Methods

ODP Site 882 lies at the western section of the Detroit Seamounts (50°22'N, 167°36'E) in the open waters of the northwest Pacific Ocean at a water depth of 3,244 m (Figure 1). Samples from 2.85 to 2.55 Ma that have previously been analyzed for diatom $\delta^{18}\text{O}$ ($\delta^{18}\text{O}_{\text{diatom}}$) and $\delta^{30}\text{Si}$ ($\delta^{30}\text{Si}_{\text{diatom}}$; Bailey et al., 2011; Haug et al., 2005; Swann, 2010; Swann et al., 2006), using an age model derived from the astronomical calibration of high resolution GRAPE density and magnetic susceptibility measurements (Tiedemann & Haug, 1995), were reanalyzed for $\delta^{13}\text{C}_{\text{diatom}}$. Samples were previously cleaned and prepared for isotope analysis using standard methodologies for diatom isotope research involving chemical treatment with H_2O_2 , HCl, and sieving with sample purity confirmed through light microscopy and scanning electron microscopy (see Swann et al., 2006, for full details). All analyzed samples originated from the 75 to 150 μm fraction and are exceptionally well preserved with no signs of dissolution. This fraction is dominated by two taxa, *Coscinodiscus marginatus* (Ehrenb.) and *Coscinodiscus radiatus* (Ehrenb.), with *C. marginatus* dominating (approximately >90% relative biovolume abundance) until after the development of the halocline at 2.73 Ma when *C. radiatus* becomes dominant (see supporting information Table S1; Figure 2). Blooms of *C. marginatus* and *C. radiatus* occur through the year with elevated fluxes in autumn/early winter (Onodera et al., 2005; Takahashi, 1986; Takahashi et al., 1996). Consequently, the diatom isotope data obtained here are interpreted as primarily reflecting annually averaged conditions with a slight bias toward autumn/early winter months. All $\delta^{13}\text{C}_{\text{diatom}}$ analyses were completed using a Costech elemental analyzer linked to an Optima mass spectrometer via cold trapping at the Natural Environment Research Council Isotope Geoscience Facility at the British Geological Survey (Hurrell et al., 2011).

A number of low-resolution foraminifera $\delta^{13}\text{C}$ records exist at ODP Site 882 over the iNHG (Maslin et al., 1996) and so can be used to monitor the $\delta^{13}\text{C}$ of the HCO_3^- substrate. For the purpose of this study only the planktonic *Globigerina bulloides* record is used due to its tendency to mainly calcify in the uppermost section of the water column at depths similar to the analyzed diatom taxa. For example, data from other available planktonic taxa, including *Neogloboquadrina pachyderma* (right plus left coiling), are not comparable to $\delta^{13}\text{C}_{\text{diatom}}$ due to their scarcity in the sediment record and/or due to their potential to calcify at lower depths outside the photic zone. In an attempt to increase the resolution of the *G. bulloides* record, additional samples were picked where possible and analyzed using an Isoprime Multiprep system attached to a GV Isoprime dual-inlet mass spectrometer as a tracer of $\delta^{13}\text{C}_{\text{DIC}}$. All $\delta^{13}\text{C}_{\text{diatom}}$ and $\delta^{13}\text{C}_{\text{foram}}$ values are expressed on the V-PDB scale by reference to an internal laboratory standard calibrated against NBS-19 and NBS-22.

Other records from ODP Site 882 that are relevant to this study include estimates of sea surface salinity (SSS; $\delta^{18}\text{O}_{\text{diatom}}$) and sea surface temperature (SST; U_{37}^k ; Haug et al., 2005; Swann, 2010; Swann et al., 2006), which are required for calculating K_H in equation (8). Values of $p\text{CO}_{2(\text{aq})}$ were reconstructed following equations (1)–(8) using interpolated values of $\delta^{13}\text{C}_{\text{foram}}$, SST, and SSS with $\delta^{13}\text{C}_{\text{foram}}$ measurements corrected for their offset from $\delta^{13}\text{C}_{\text{DIC}}$ following Spero and Lea (1996). Estimates of b were derived using existing opal concentrations data (Haug et al., 1999; Sigman et al., 2004) and calibrations for b published in Stoll et al. (2017) for centric taxa ($R^2 = 0.86$, $p < 0.01$). The uncertainty associated with b and $p\text{CO}_{2(\text{aq})}$ was calculated using Monte Carlo simulations (10,000 replicates) with the Monte Carlo package in R (Leschinski, 2017; R Core Team, 2017), assuming a normal distribution for proxy data uncertainty (SSS = 0.3 practical salinity unit, SST = 1.2 °C) in equations (1)–(8).

3. Results

Analytical reproducibility (1σ) from replicate analysis of sample material was 0.3‰ and <0.1‰ for $\delta^{13}\text{C}_{\text{diatom}}$ and $\delta^{13}\text{C}_{\text{foram}}$, respectively. Over the analyzed interval through the Pliocene/early Quaternary, values of

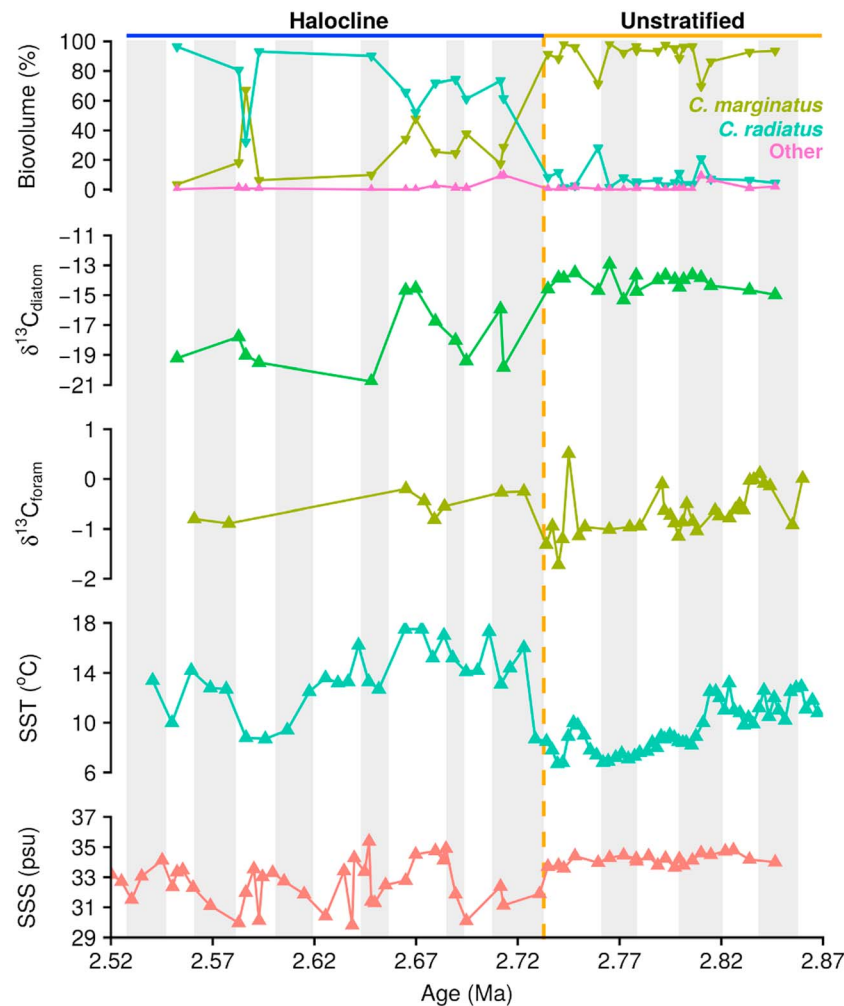


Figure 2. Late Pliocene/early Quaternary palaeoceanographic records from ODP Site 882. Changes in $\delta^{18}\text{O}_{\text{diatom}}$ derived sea surface salinity (Swann, 2010; Swann et al., 2006), U_{37}^k derived SST (Haug et al., 2005), $\delta^{13}\text{C}_{\text{foram}}$ (*G. bulloides*; Maslin et al., 1996, 1998; this study) and $\delta^{13}\text{C}_{\text{diatom}}$, used to reconstruct $p\text{CO}_{2(\text{aq})}$ (equation (1)–(9)), are compared to the relative diatom species biovolume in samples analyzed for $\delta^{13}\text{C}_{\text{diatom}}$. Orange dashed line denotes transition from unstratified to stratified water column at 2.73 Ma with gray (white) shading reflecting glacial (interglacial) intervals.

$\delta^{13}\text{C}_{\text{diatom}}$ range from -12.9‰ to -20.8‰ (Figure 2, supporting information Table S1). From 2.85 to 2.73 Ma values of $\delta^{13}\text{C}_{\text{diatom}}$ are near constant (mean = -14.1‰ , $1\sigma = 0.6\text{‰}$). Values of $\delta^{13}\text{C}_{\text{diatom}}$ then decrease for the remainder of the analyzed interval (mean = -18.0‰ , $1\sigma = 2.1\text{‰}$) in a shift that is concomitant with the marked decline in opal MAR at ODP Site 882. Through the post-iNHG interval significant variability is apparent in the $\delta^{13}\text{C}_{\text{diatom}}$ data with recurrent changes of up to 3–4‰ that do not coincide with further changes in opal MAR. Values of $\delta^{13}\text{C}_{\text{foram}}$ typically range from -0.46‰ to -0.95‰ with a shift to marginally higher values after the iNHG (Figure 2). Despite efforts to increase the resolution of the $\delta^{13}\text{C}_{\text{foram}}$ record, the number of data points declines after 2.73 Ma with sediments largely free of carbonate microfossils (Figure 2).

Values of ε_p are at or below 5 until 2.73 Ma before increasing to >5 and a mean of 8 (Figure 3). Reconstructed $p\text{CO}_{2(\text{aq})}$ at ODP Site 882 typically range from ~ 225 to 250 ppm with a peak value of 314 ppm at 2.81 Ma, a low of 192 ppm at 2.58 Ma, and mean uncertainties of 39.5 ppm (1σ ; Figure 3 and supporting information Table S1). From 2.85 to 2.73 Ma $p\text{CO}_{2(\text{aq})}$ displays a long-term decline from ~ 280 to ~ 230 ppm ($\bar{x} = 247$ ppm; $1\sigma = 25$ ppm). Thereafter, from 2.71 to 2.55 Ma, $p\text{CO}_{2(\text{aq})}$ show a marked increase in variability with fluctuation of 20–60 ppm over the interval ($\bar{x} = 225$ ppm; $1\sigma = 28$ ppm).

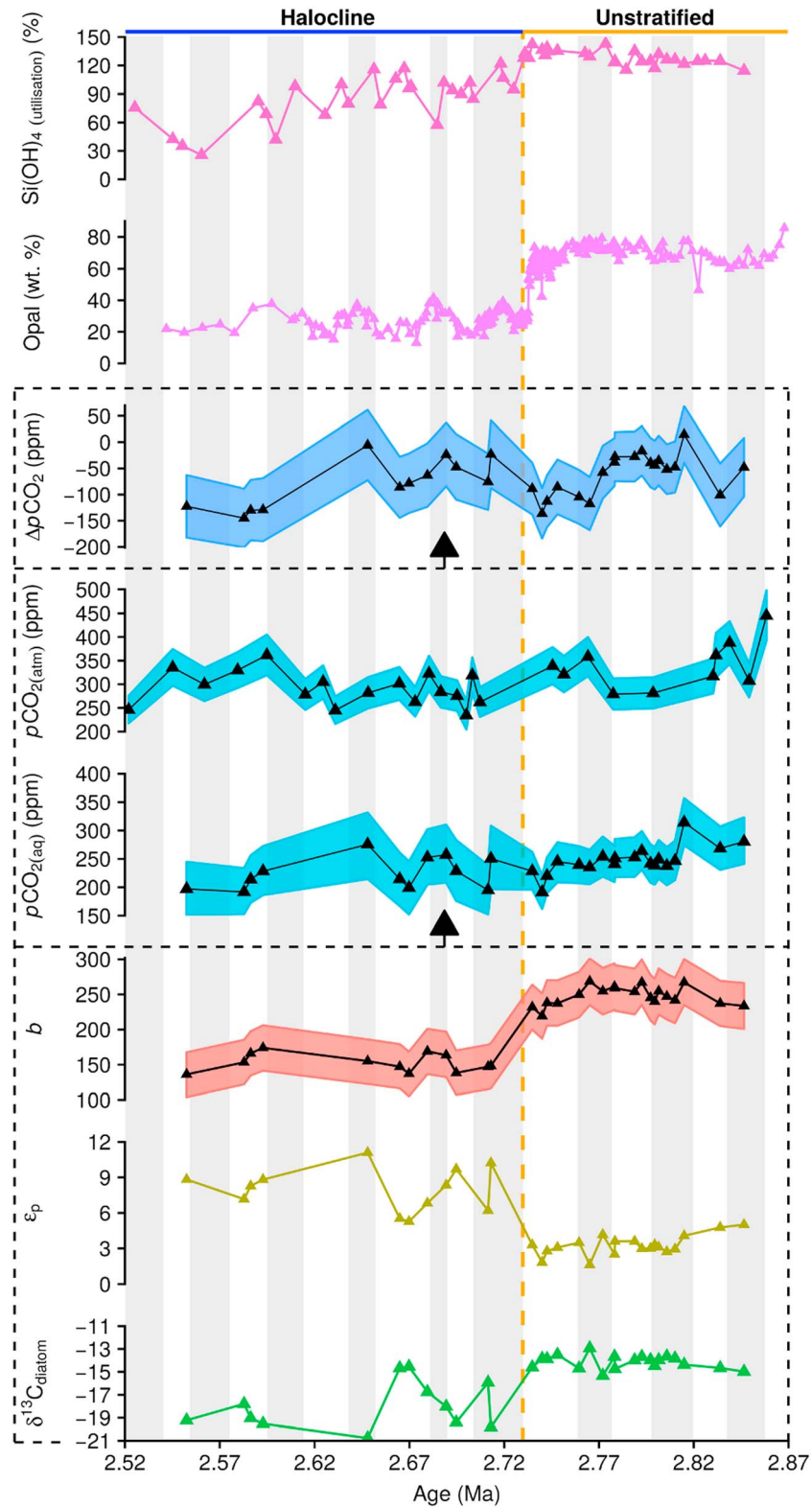


Figure 3. Temporal changes in carbon dynamics at ODP Site 882. Values of $\delta^{13}\text{C}_{\text{diatom}}$, ϵ_p , b and $p\text{CO}_2(\text{aq})$ are compared to $p\text{CO}_2(\text{atm})$ (Martinez-Boti et al., 2015) and used to calculate $\Delta p\text{CO}_2$. Shaded polygons for b , $p\text{CO}_2(\text{aq})$, $p\text{CO}_2(\text{atm})$, and $\Delta p\text{CO}_2$ reflect the 1σ uncertainty derived from Monte Carlo simulations. Changes in opal concentrations (Haug et al., 1999; Sigman et al., 2004) and rates of $\text{Si}(\text{OH})_4$ utilization (Swann et al., 2016) provide information on the biological pump and the export of carbon into the ocean interior. Orange dashed line denotes transition from unstratified to stratified water column at 2.73 Ma with gray (white) shading reflecting glacial (interglacial) intervals.

4. Discussion

4.1. Changes in Photic Zone $p\text{CO}_{2(\text{aq})}$

High values of $\delta^{30}\text{Si}_{\text{diatom}}$ and opal MAR from 2.85 to 2.73 Ma indicate significant upwelling of nutrient-rich subsurface waters, which resulted in a productive water column marked by high rates of silicic acid $[\text{Si}(\text{OH})_4]$ utilization (Bailey et al., 2011; Haug et al., 1999; Reynolds et al., 2008; Sigman et al., 2004; Swann et al., 2016; Figure 3). This situation contrasts with the post-2.73 Ma interval when the development of a halocline ceased significant upwelling and led to associated reductions in $\text{Si}(\text{OH})_4$ utilization and siliceous productivity (Haug et al., 1999, 2005; Reynolds et al., 2008; Sigman et al., 2004; Swann et al., 2006, 2016; Figure 3). The presence of lower $p\text{CO}_{2(\text{aq})}$ after 2.73 Ma is consistent with these palaeoceanographic changes, namely, a reduction in deeper CO_2 -rich waters reaching the photic zone under conditions of enhanced near-surface stratification. On this basis, the increased variability of $p\text{CO}_{2(\text{aq})}$ after 2.73 Ma may reflect changes in the strength of this stratification, an event which might impact the advection of carbon and nutrient-rich deep water supply to the photic zone and so rates of $\text{Si}(\text{OH})_4$ utilization. However, before and after the establishment of the halocline at 2.73 Ma, changes in $p\text{CO}_{2(\text{aq})}$ show no relationship to rates of $\text{Si}(\text{OH})_4$ utilization, SSS or SST (Figure 3).

4.2. Implications for Ocean Ventilation Over the iNHG

To establish whether changes in subarctic Pacific $p\text{CO}_{2(\text{aq})}$ resulted in the region acting as a net sink or source of CO_2 , comparisons are needed to estimates of global $p\text{CO}_{2(\text{atm})}$. A number of modeled and proxy-based records have been published in recent years, but here we focus our comparisons on a recent multisite $\delta^{11}\text{B}$ record, which is the highest-resolution record to date and displays a decline in $p\text{CO}_{2(\text{atm})}$ of 40–90 ppm through the late Pliocene/early Pleistocene interval (Martinez-Boti et al., 2015). Calculation of $\Delta p\text{CO}_2$ (equation (9)) between all $\delta^{13}\text{C}_{\text{diatom}}$ derived $p\text{CO}_{2(\text{aq})}$ at ODP Site 882 and interpolated $p\text{CO}_{2(\text{atm})}$ reveals considerable variation over the analyzed interval (Figure 3). The mean age difference between the interpolated and original $p\text{CO}_{2(\text{atm})}$ data is 4.3 ka ($1\sigma = 3.7$ ka). With the exception of one sample at 2.81 Ma, values of $\Delta p\text{CO}_2$ are negative throughout the analyzed interval ($\bar{x} = -68$ ppm; $1\sigma = 43$ ppm). While $\Delta p\text{CO}_2$ is lower after the development of the halocline at 2.73 Ma (pre-2.73 Ma: $\bar{x} = -61$ ppm; $1\sigma = 40$ ppm; post-2.73 Ma: $\bar{x} = -78$ ppm; $1\sigma = 47$ ppm), consistent with reduced upwelling of deep waters to the photic zone, this change is not significant ($p = 0.2$). The lack of a systematic shift in mean $\Delta p\text{CO}_2$ values after 2.73 Ma can be attributed to the large variations in both $p\text{CO}_{2(\text{aq})}$ and $\Delta p\text{CO}_2$ post-iNHG. More significantly, the results cast doubt on the notion that changes in the regional carbon dynamics in the subarctic Pacific Ocean played a key role in driving the iNHG. Although there is considerable variability in estimates of late Pliocene $p\text{CO}_{2(\text{atm})}$ both within and between individual studies (e.g., Badger et al., 2013; Bartoli et al., 2011; Martinez-Boti et al., 2015; Pagani et al., 2010; Seki et al., 2010; Stap et al., 2016; van de Wal et al., 2011; Willeit et al., 2015) in all cases reconstructed values of $p\text{CO}_{2(\text{atm})}$ remain above typical values of $p\text{CO}_{2(\text{aq})}$ at ODP Site 882. Values of $\Delta p\text{CO}_2$ at ODP Site 882 remains predominantly negative even when considering the Monte Carlo-derived uncertainties for both $p\text{CO}_{2(\text{aq})}$ and $p\text{CO}_{2(\text{atm})}$ (Figure 3).

Consistently low values of $\Delta p\text{CO}_2$ from 2.85 to 2.73 Ma suggest that the mixed water column that prevailed in the Pliocene prior to stratification did not release significant volumes of CO_2 to the atmosphere and so did not help maintain the warm Pliocene climate state. This interval in the ODP Site 882 record is marked by exceptional high opal concentrations of circa 60–75% ($\sim 2.2\text{--}3.2 \text{ g}\cdot\text{cm}^{-2}\cdot\text{ka}^{-1}$; Haug et al., 1999) and rates of $\text{Si}(\text{OH})_4$ utilization (Swann et al., 2016; Figure 3). Consequently, although the mixed water column in this interval would have led to increased delivery of carbon rich waters to the surface, the negative values of $\Delta p\text{CO}_2$ suggest that the associated flux of nutrients to the photic zone enabled a highly efficient biological pump that prevented carbon release from the ocean to the atmosphere (Figure 3, 4a). We note, however, that this scenario is not supported by comparisons to the modern day where regions of strong upwelling and high diatom productivity/export remain net sources of CO_2 to the atmosphere (Takahashi et al., 2009, 2016). The uncertainties in using $\delta^{13}\text{C}_{\text{diatom}}$ to reconstruct $p\text{CO}_{2(\text{aq})}$ are discussed in section 4.3. While these indicate the issues in quantifying $p\text{CO}_{2(\text{aq})}$ and $\Delta p\text{CO}_2$ from $\delta^{13}\text{C}_{\text{diatom}}$, thereby potentially explaining the anomalous negative values of $\Delta p\text{CO}_2$ at ODP Site 882, the underlying trends in $p\text{CO}_{2(\text{aq})}$ and $\Delta p\text{CO}_2$ can be used to understand regional late Pliocene/early Quaternary carbon dynamics in the subarctic Pacific. Although the development of the halocline at 2.73 Ma lowered $p\text{CO}_{2(\text{aq})}$ in line with reduced deep water upwelling, the

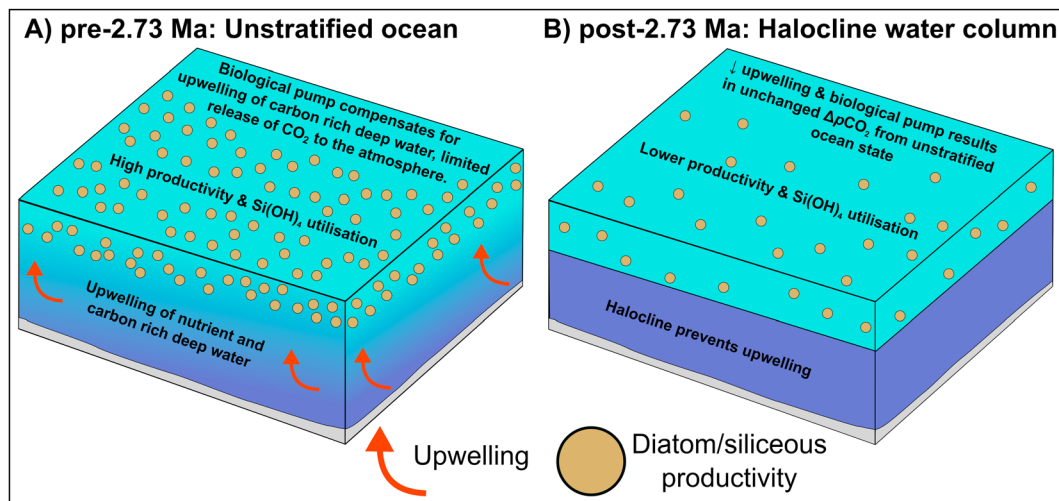


Figure 4. Conceptual model of the palaeoceanographic changes in the northwest subarctic Pacific Ocean. (a) From 2.85 to 2.73 Ma an unstratified water column leads to unimpeded upwelling of deep water. The transportation of nutrients and carbon rich waters to the photic zone is compensated by high levels of siliceous productivity and Si(OH)₄ utilisation creating a highly efficient biological pump that minimizes CO₂ leakage to the atmosphere. (b) Following the development of the halocline, deep waters are limited from reaching the photic zone. The corresponding decline in both the strength and efficiency of the biological pump, however, results in the net ocean atmospheric flux of CO₂ remaining similar to conditions prior to 2.73 Ma with only minor decreases in $p\text{CO}_{2(\text{aq})}$ and $\Delta p\text{CO}_2$.

absence of a bigger decline in $p\text{CO}_{2(\text{aq})}$ as well as $\Delta p\text{CO}_2$ is unexpected. After 2.73 Ma, opal concentration fall to ~20–33% ($\sim 0.5\text{--}1.0\text{ g}\cdot\text{cm}^{-2}\cdot\text{ka}^{-1}$; Haug et al., 1999; Sigman et al., 2004) with corresponding declines in silicic acid utilization (Swann et al., 2016; Figure 3). We argue that a decline in Si(OH)₄ utilization and the efficiency of biological export of carbon balanced out the reduced rate at which deep water carbon was advected to the photic zone, preventing a major decline in $p\text{CO}_{2(\text{aq})}$ or the net flux of CO₂ across the ocean-atmosphere interface ($\Delta p\text{CO}_2$; Figure 4b).

A number of models have indicated that a decline in $p\text{CO}_{2(\text{atm})}$ is critical for the development of large Northern Hemisphere ice sheets (e.g., Lunt et al., 2008). With evidence presented here that carbon dynamics and $\Delta p\text{CO}_2$ did not significantly change in the subarctic North Pacific Ocean over the iNHG, the focus shifts to the Southern Ocean which plays a key role in regulating the ~100 ppm variations in $p\text{CO}_{2(\text{atm})}$ over Pleistocene glacial-interglacial cycles (Sigman et al., 2010). Evidence for changes in Antarctic ice sheet extent together with variations in Southern Ocean sea ice and stratification through the Pliocene and oNHG (Hillenbrand & Cortese, 2006; Hodell & Venz-Curtis, 2006; McKay et al., 2012; Naish et al., 2009; Waddell et al., 2009) could have enhanced the ability of the Southern Ocean to act as a sink of atmospheric $p\text{CO}_{2(\text{atm})}$ through mechanisms that are analogous to those that occur in the Pleistocene (see Sigman et al., 2010). These processes could have been strengthened by increased eolian iron deposition in the Southern Ocean over this interval, which would have increased the efficiency of the biological pump and the sequestration of carbon into the ocean interior (Martínez-García et al., 2011).

4.3. Uncertainties With $\delta^{13}\text{C}_{\text{diatom}}$

Despite measurements of $\delta^{13}\text{C}_{\text{diatom}}$ having been used in palaeoenvironmental reconstructions for over a decade to examine changes in photosynthetic carbon demand/productivity, its use to reconstruct $p\text{CO}_{2(\text{aq})}$ is relatively novel. Consequently, a discussion of the potential errors/limitations with $\delta^{13}\text{C}_{\text{diatom}}$ is appropriate to place the reconstructions of $p\text{CO}_{2(\text{aq})}$ at ODP Site 882 into a wider context.

4.3.1. Diatom Carbon Uptake

In contrast to foraminifera formed via the precipitation of HCO_3^- , diatoms uptake carbon from both HCO_3^- and $\text{CO}_{2(\text{aq})}$ through carbon concentrating mechanisms (CCM) that enable the saturation of the enzyme RuBisCO that catalyzes carbon fixation (Tortell et al., 1997). Such processes primarily involve either an active, direct, transportation of HCO_3^- , and $\text{CO}_{2(\text{aq})}$ into the cell or an indirect HCO_3^- uptake in which an extracellular carbonic anhydrase dehydrates HCO_3^- to CO₂ (Badger, 2003; Sültmeyer et al., 1993). In addition to these C₃ photosynthetic pathways, an indirect C₄ pathway has also been identified in which HCO_3^- is

converted to malic or aspartic acid and then to CO_2 by decarboxylation (Reinfelder et al., 2000, 2004; Roberts et al., 2007).

Results from the Bering Sea, North Pacific, Equatorial Pacific, and Southern Oceans show that significant, but variable, amounts of diatom carbon originates from HCO_3^- with the majority of this occurring via direct transportation (Cassar et al., 2004; Martin & Tortell, 2006; Tortell et al., 2006, 2008, 2010; Tortell & Morel, 2002). Although $\text{HCO}_3^-:\text{CO}_{2(\text{aq})}$ uptake ratios may vary with large changes in pH (Trimborn et al., 2008) and interspecies variations in cell morphologies (Martin & Tortell, 2008), others have shown that this ratio does not change with $p\text{CO}_{2(\text{aq})}$, Fe availability, growth rates, primary productivity, or frustule area:volume ratios (Cassar et al., 2004; Martin & Tortell, 2006; Tortell et al., 2006, 2008). The results presented here from ODP Site 882 do not account for any isotopic offset that may arise over the usage of HCO_3^- over CO_2 or the potential for active carbon uptake to alter ϵ_p (Burkhardt et al., 2001). For example, increases in $p\text{CO}_{2(\text{aq})}$ have been shown to downregulate CCM (Hennon et al., 2015), introducing a nonlinear relationship between ϵ_p and $\delta^{13}\text{C}_{\text{diatom}}$, which impacts the ability to accurately reconstruct changes in $p\text{CO}_{2(\text{aq})}$ (Laws et al., 2002; Raven et al., 2011). Although these issues may impact the absolute values of reconstructed $p\text{CO}_{2(\text{aq})}$, we feel confident given the points made above that changes in $\text{HCO}_3^-:\text{CO}_2$ uptake ratios and transportation mechanism have not significantly altered over the analyzed interval or impacted the underlying trends in $p\text{CO}_{2(\text{aq})}$ and our assertion that the development of the halocline did not fundamentally alter regional carbon dynamics across the iNHG. For example, attempts to reconstruct $p\text{CO}_{2(\text{aq})}$ over the last 14 Ma using models that accounts for diffusive and active uptake of CO_2 by CCM results in different absolute values of $p\text{CO}_{2(\text{aq})}$ but similar temporal trends (Mejía et al., 2017).

4.3.2. Physiological Factors

Physiological controls on the diffusion and fractionation of carbon into diatom, summarized by the term b (equation (7)), may change and alter $\delta^{13}\text{C}_{\text{diatom}}$ in response to different forms of RuBisCO, amino acids, growth rates, cell morphology, and CCM (Cassar et al., 2006; Laws et al., 1995, 2002; Rau et al., 1996, 1997, 2001; Rosenthal et al., 2000; Scott et al., 2007), which in turn are potentially linked to evidence of a possible interspecies isotope vital effects in fossil measurements of $\delta^{13}\text{C}_{\text{diatom}}$ (Jacot des Combes et al., 2008).

Within the context of this study the impact of isotope vital effects, other symbiont/physiological processes such as diatom cell size, geometry as well as the aforementioned $\text{HCO}_3^-:\text{CO}_2$ uptake process (Jacot des Combes et al., 2008; Laws et al., 1995, 1997; Martin & Tortell, 2008; Popp et al., 1998) can be partially circumvented by the use of a single size fraction of diatoms, dominated by only two taxa (supporting information Table S1). This point is emphasized from 2.85 to 2.73 Ma when analyzed samples are dominated by *C. marginatus* (>90% relative abundance) and high nutrient concentrations would have created near-steady photic zone growth rates. While declines in $\delta^{13}\text{C}_{\text{diatom}}$ and b as well as increases in ϵ_p coincide at 2.73 Ma with a change from *C. marginatus* to *C. radiatus* dominance in the analyzed samples, we attribute this change to the development of the regional halocline, with concordant changes in SST, SSS, and opal concentrations, rather than an interspecies vital effect process (Figures 2 and 3). While modern samples/culture experiments are needed to fully confirm the absence of an interspecies vital effect, we note that values of $\delta^{13}\text{C}_{\text{diatom}}$ both before ($R^2 = 0.01$) and after 2.73 Ma ($R^2 = -0.12$) are not related to the relative abundance of either *C. marginatus* or *C. radiatus* despite notable variation in the populations of both taxa in each interval (supporting information Table S1). Finally, to fully account for physiological processes and reconstruct $p\text{CO}_2$ from $\delta^{13}\text{C}_{\text{diatom}}$, accurate estimates of b are required. Some previous studies have primarily based $p\text{CO}_2$ reconstructions from diatoms on growth rates (μ ; e.g., Heurreux & Rickaby, 2015; Rosenthal et al., 2000). Here we elect to directly constrain b based on the results of a Southern Ocean core-top study between the Polar Front and Southern Antarctic Circumpolar Current Front (Stoll et al., 2017). Despite calibrations being statistically significant, the standard error associated with this calibration results in a large uncertainty with the estimates of b used in this study ($1\sigma = 32.3 \pm 0.5$). This, in turn, is the main source of the uncertainty derived in the Monte Carlo simulations for $p\text{CO}_{2(\text{aq})}$ (Figure 3). It also remains unknown to what extent the Southern Ocean calibration of b can be directly applied elsewhere in the global ocean, to different taxa and/or through the geological record (Stoll et al., 2017), although these calibrations have been used on samples back to the Miocene (Mejía et al., 2017).

4.3.3. Underestimation of $p\text{CO}_{2(\text{aq})}$

In addition to the discussion above, we note that the reconstructed values of $p\text{CO}_{2(\text{aq})}$ (173–288 ppm) are considerably lower than modern values of $p\text{CO}_{2(\text{aq})}$ (331–408 μatm) from 50°–50.5°N and 167°–168°E that have been collected over the past two decades in different seasons (Takahashi et al., 2016). The low values are also reflected in the reconstructed values of $\Delta p\text{CO}_2$ over the analyzed interval (+15 to –145 ppm; $x^- = -68$ ppm; $1\sigma = 43$ ppm). In contrast, modern monthly $\Delta p\text{CO}_2$ from the region range from –50 to +44 μatm (Takahashi et al., 2009) with mean annual preindustrial $\Delta p\text{CO}_2 + 3$ ppm ($p\text{CO}_{2(\text{aq})} \sim 280$ ppm; $p\text{CO}_{2(\text{atm})} \sim 277$; Japan Agency for Marine-Earth Science and Technology; Atmosphere and Ocean Research Institute; Centre for Climate System Research-National Institute for Environmental Studies, 2013). Although comparing modern and palaeo-estimates of $p\text{CO}_{2(\text{aq})}$ and $\Delta p\text{CO}_2$ is problematic given the storage of anthropogenic carbon and warming SST in the modern marine system, these lines of evidences suggest that our $\delta^{13}\text{C}_{\text{diatom}}$ reconstruction might underestimate the true values of $p\text{CO}_{2(\text{aq})}$ and $\Delta p\text{CO}_2$ at ODP Site 882 through the late Pliocene/early Quaternary. While part of this underestimation may relate to differences in $p\text{CO}_{2(\text{aq})}$ seasonality before/after the development of the halocline, the impact of this is likely to be less than the Monte Carlo inferred uncertainty of the $p\text{CO}_{2(\text{aq})}$ reconstruction (mean uncertainty = 39.5 ppm; see Supplementary Table 1). Given the limited work conducted to date on diatom b and its identification above as the main source of uncertainty in reconstructing $p\text{CO}_{2(\text{aq})}$ in this study, we suggest that further calibrations of this parameter are needed outside of the Southern Ocean and involving a greater range of taxa. Notwithstanding this issue, based on current knowledge we remain confident in the overall trend and magnitude of change in our reconstructed record of $p\text{CO}_{2(\text{aq})}$ and $\Delta p\text{CO}_2$. As such, we reiterate our main finding that the development of the halocline in the subarctic northwest Pacific Ocean at 2.73 Ma did not lead to a major change in regional marine-atmospheric fluxes of CO_2 and that therefore carbon dynamics in the region did not play a major role in aiding the iNHG.

5. Conclusions

Understanding the potential sources and sinks of atmospheric CO_2 that helped regulate the global climate through the late Pliocene is of critical importance given the interval's potential to act as an analog for a warmer climate state in the 21st century and beyond. New results based on $\delta^{13}\text{C}_{\text{diatom}}$ from ODP Site 882 in the northwest subarctic Pacific Ocean show that regional ocean atmospheric exchanges of CO_2 did not fundamentally alter over the iNHG. This occurred despite a reduction in the upwelling of high- $p\text{CO}_{2(\text{aq})}$ deep waters at 2.73 Ma that were balanced by a corresponding reduction in carbon export by a less efficient biological pump. While uncertainties exist in using $\delta^{13}\text{C}_{\text{diatom}}$ to reconstruct $p\text{CO}_{2(\text{aq})}$ and $\Delta p\text{CO}_2$, highlighting the need for more modern calibrations in particular for the term b , the results suggest that any decline in $p\text{CO}_{2(\text{atm})}$ through the late Pliocene and early Quaternary was not driven by changes in the northwest subarctic Pacific Ocean.

Acknowledgments

Supporting data ($\delta^{13}\text{C}_{\text{diatom}}$ and $p\text{CO}_{2(\text{aq})}$) data together with the diatom species composition of analyzed samples from ODP Site 882 between 2.85 and 2.55 Ma) are included as a spreadsheet in the supporting information. This work was supported by the Natural Environment Research Council and a NERC postdoctoral fellowship award to GEAS (grants NE/F012969/1 and NE/F012969/2). We thank the staff at the IODP Gulf Coast Core Repository for providing samples and sampling cores from ODP Site 882 in addition to Carol Arrowsmith for assistance with the $\delta^{13}\text{C}_{\text{diatom}}$ analyses and Hilary Sloane for analyzing the additional planktonic $\delta^{13}\text{C}_{\text{foram}}$ samples. Finally, thanks are owed to the two anonymous reviewers and the Editor (Stephen Barker) whose comments significantly improved the manuscript.

References

- Badger, M. (2003). The roles of carbonic anhydrases in photosynthetic CO_2 concentrating mechanisms. *Photosynthesis Research*, 77(2/3), 83–94. <https://doi.org/10.1023/A:1025821717773>
- Badger, M. P. S., Schmidt, D. N., Mackensen, A., & Pancost, R. D. (2013). High-resolution alkenone palaeobarometry indicates relatively stable $p\text{CO}_2$ during the Pliocene (3.3–2.8 Ma). *Philosophical Transactions of the Royal Society A: Mathematical, Physical and Engineering Sciences*, 371(2001), 20130094. <https://doi.org/10.1098/rsta.2013.0094>
- Bai, Y.-J., Chen, L.-Q., Ranhotra, P., Wang, Q., Wang, Y.-F., & Li, C.-S. (2015). Reconstructing atmospheric CO_2 during the Plio-Pleistocene transition by fossil *Typha*. *Global Change Biology*, 21(2), 874–881. <https://doi.org/10.1111/gcb.12670>
- Bailey, I., Hole, G. M., Foster, G. L., Wilson, P. A., Storey, C. D., Trueman, C. N., & Raymo, M. E. (2013). An alternative suggestion for the Pliocene onset of major northern hemisphere glaciation based on the geochemical provenance of North Atlantic Ocean ice-rafted debris. *Quaternary Science Reviews*, 75, 181–194. <https://doi.org/10.1016/j.quascirev.2013.06.004>
- Bailey, I., Liu, Q., Swann, G. E. A., Jiang, Z., Sun, Y., Zhao, X., & Roberts, A. P. (2011). Iron fertilisation and biogeochemical cycles in the sub-Arctic Northwest Pacific during the late Pliocene intensification of northern hemisphere glaciation. *Earth and Planetary Science Letters*, 307(3–4), 253–265. <https://doi.org/10.1016/j.epsl.2011.05.029>
- Bartoli, G., Hönisch, B., & Zeebe, R. E. (2011). Atmospheric CO_2 decline during the Pliocene intensification of Northern Hemisphere glaciations. *Paleoceanography*, 26, PA4213. <https://doi.org/10.1029/2010PA002055>
- Bidigare, R. R., Fluegge, A., Freeman, K. H., Hanson, K. L., Hayes, J. M., Hollander, D., et al. (1997). Consistent fractionation of ^{13}C in nature and in the laboratory: Growth-rate effects in some haptophyte algae. *Global Biogeochemical Cycles*, 11, 279–292. <https://doi.org/10.1029/96GB03939>
- Bonelli, S., Charbit, S., Kageyama, M., Woillez, M.-N., Ramstein, G., Dumas, C., & Quiquet, A. (2009). Investigating the evolution of major Northern Hemisphere ice sheets during the last glacial-interglacial cycle. *Climate of the Past*, 5(3), 329–345. <https://doi.org/10.5194/cp-5-329-2009>

- Brierley, C. M., & Fedorov, A. V. (2016). Comparing the impacts of Miocene–Pliocene changes in inter-ocean gateways on climate: Central American seaway, Bering Strait, and Indonesia. *Earth and Planetary Science Letters*, 444, 116–130. <https://doi.org/10.1016/j.epsl.2016.03.010>
- Burkhardt, S., Amoroso, G., Riebesell, U., & Sültemeyer, D. (2001). CO₂ and HCO₃[−] uptake in marine diatoms acclimated to different CO₂ concentrations. *Limnology and Oceanography*, 46, 1378–1391. <https://doi.org/10.4319/lo.2001.46.6.1378>
- Cassar, N., Laws, E. A., Bidigare, R. R., & Popp, B. N. (2004). Bicarbonate uptake by Southern Ocean phytoplankton. *Global Biogeochemical Cycles*, 18, GB2003. <https://doi.org/10.1029/2003GB002116>
- Cassar, N., Laws, E. A., & Popp, B. N. (2006). Carbon isotopic fractionation by the marine diatom *Phaeodactylum tricornutum* under nutrient- and light-limited growth conditions. *Geochimica et Cosmochimica Acta*, 70(21), 5323–5335. <https://doi.org/10.1016/j.gca.2006.08.024>
- Chierici, M., Fransson, A., & Nojiri, Y. (2006). Biogeochemical processes as drivers of surface fCO₂ in contrasting provinces in the subarctic North Pacific Ocean. *Global Biogeochemical Cycles*, 20, GB1009. <https://doi.org/10.1029/2004GB002356>
- Driscoll, N. W., & Haug, G. H. (1998). A short cut in thermohaline circulation: A cause for Northern Hemisphere glaciation? *Science*, 282(5388), 436–438. <https://doi.org/10.1126/science.282.5388.436>
- Foster, G. L., & Rae, J. W. B. (2016). Reconstructing ocean pH with boron isotopes in foraminifera. *Annual Review of Earth and Planetary Sciences*, 44(1), 207–237. <https://doi.org/10.1146/annurev-earth-060115-012226>
- Frank, D. C., Esper, J., Raible, C. C., Buntgen, U., Trouet, V., Stocker, B., & Joos, F. (2010). Ensemble reconstruction constraints on the global carbon cycle sensitivity to climate. *Nature*, 463(7280), 527–530. <https://doi.org/10.1038/nature08769>
- Haug, G. H., Ganopolski, A., Sigman, D. M., Rosell-Mele, A., Swann, G. E. A., Tiedemann, R., et al. (2005). North Pacific seasonality and the glaciation of North America 2.7 million years ago. *Nature*, 433(7028), 821–825. <https://doi.org/10.1038/nature03332>
- Haug, G. H., Sigman, D. M., Tiedemann, R., Pedersen, T. F., & Sarnthein, M. (1999). Onset of permanent stratification in the subarctic Pacific Ocean. *Nature*, 401(6755), 779–782. <https://doi.org/10.1038/44550>
- Haug, G. H., & Tiedemann, R. (1998). Effect of the formation of the Isthmus of Panama on Atlantic Ocean thermohaline circulation. *Nature*, 393(6686), 673–676. <https://doi.org/10.1038/31447>
- Hecky, R. E., Mopper, K., Kilham, P., & Degens, E. T. (1973). The amino acid and sugar composition of diatom cell-walls. *Marine Biology*, 19(4), 323–331. <https://doi.org/10.1007/BF00348902>
- Hennon, G. M. M., Ashworth, J., Groussman, R. D., Berthiaume, C., Morales, R. L., Baliga, N. S., et al. (2015). Diatom acclimation to elevated CO₂ via cAMP signalling and coordinated gene expression. *Nature Climate Change*, 5(8), 761–765. <https://doi.org/10.1038/nclimate2683>
- Heureux, A. M. C., & Rickaby, R. E. M. (2015). Refining our estimate of atmospheric CO₂ across the Eocene–Oligocene climatic transition. *Earth and Planetary Science Letters*, 409, 329–338. <https://doi.org/10.1016/j.epsl.2014.10.036>
- Hillenbrand, C.-D., & Cortese, G. (2006). Polar stratification: A critical view from the Southern Ocean. *Palaeogeography, Palaeoclimatology, Palaeoecology*, 242(3–4), 240–252. <https://doi.org/10.1016/j.palaeo.2006.06.001>
- Hodell, D. A., & Venz-Curtis, K. A. (2006). Late Neogene history of deepwater ventilation in the Southern Ocean. *Geochemistry, Geophysics, Geosystems*, 7(9), Q09001. <https://doi.org/10.1029/2005GC001211>
- Honda, M. C., Imai, K., Nojiri, Y., Hoshi, F., Sugawara, T., & Kusakabe, M. (2002). The biological pump in the northwestern North Pacific based on fluxes and major components of particulate matter obtained by sediment-trap experiments (1997–2000). *Deep Sea Research, Part II*, 49(24–25), 5595–5625. [https://doi.org/10.1016/S0967-0645\(02\)00201-1](https://doi.org/10.1016/S0967-0645(02)00201-1)
- Hurrell, E. R., Barker, P. A., Leng, M. J., Vane, C. H., Wynn, P., Kendrick, C. P., et al. (2011). Developing a methodology for carbon isotope analysis of lacustrine diatoms. *Rapid Communications in Mass Spectrometry*, 25(11), 1567–1574. <https://doi.org/10.1002/rcm.5020>
- Jacot des Combes, H., Esper, O., De La Rocha, C. L., Abelman, A., Gersonde, R., Yam, R., & Shemesh, A. (2008). Diatom δ¹³C, δ¹⁵N, and C/N since the Last Glacial Maximum in the Southern Ocean: Potential impact of species composition. *Paleoceanography*, 23, PA4209. <https://doi.org/10.1029/2008PA001589>
- Japan Agency for Marine–Earth Science and Technology; Atmosphere and Ocean Research Institute; Centre for Climate System Research–National Institute for Environmental Studies (2013): WCRP CMIP5: The MIROC team MIROC-ESM model output collection. Centre for Environmental Data Analysis, 26th February 2018. Retrieved from <http://catalogue.ceda.ac.uk/uuid/bf3c7e63092b45f2927e3e1d260c4f01>
- Kleiven, H. F., Jansen, E., Fronval, T., & Smith, T. M. (2002). Intensification of Northern Hemisphere glaciations in the circum Atlantic region (3.5–2.4 Ma)—Ice-rafted detritus evidence. *Palaeogeography Palaeoclimatology Palaeoecology*, 184(3–4), 213–223. [https://doi.org/10.1016/S0031-0182\(01\)00407-2](https://doi.org/10.1016/S0031-0182(01)00407-2)
- Kröger, N., Deutzmann, R., Bergsdorf, C., & Sumper, M. (2000). Species-specific polyamines from diatoms control silica morphology. *Proceedings of the National Academy of Sciences of the United States of America*, 97(26), 14,133–14,138. <https://doi.org/10.1073/pnas.260496497>
- Kröger, N., Deutzmann, R., & Sumper, M. (1999). Polycationic peptides from diatom biosilica that direct silica nanosphere formation. *Science*, 286(5442), 1129–1132.
- Lauvset, S. K., Key, R. M., Olsen, A., van Heuven, S., Velo, A., Lin, X., et al. (2016). A new global interior ocean mapped climatology: The 1° × 1° GLODAP version 2. *Earth System Science Data*, 8, 325–340.
- Laws, E. A., Bidigare, R. R., & Popp, B. N. (1997). Effect of growth rate and CO₂ concentration on carbon isotope fractionation by the marine diatom *Phaeodactylum tricornutum*. *Limnology and Oceanography*, 42(7), 1552–1560. <https://doi.org/10.4319/lo.1997.42.7.1552>
- Laws, E. A., Popp, B. N., Bidigare, R. R., Kennicutt, M. C., & Macko, S. A. (1995). Dependence of phytoplankton carbon isotopic composition on growth rate and [CO₂]_{aq}: Theoretical considerations and experimental results. *Geochimica et Cosmochimica Acta*, 59(6), 1131–1138. [https://doi.org/10.1016/0016-7037\(95\)00030-4](https://doi.org/10.1016/0016-7037(95)00030-4)
- Laws, E. A., Popp, B. N., Cassar, N., & Tanimoto, J. (2002). ¹³C discrimination patterns in oceanic phytoplankton: Likely influence of CO₂ concentrating mechanisms, and implications for palaeoreconstructions. *Functional Plant Biology*, 29(3), 323–333. <https://doi.org/10.1071/PP01183>
- Leschinski, C. H. (2017). MonteCarlo: Automatic parallelized Monte Carlo simulations. R package version 1.0.2. Retrieved from <https://CRAN.R-project.org/package=MonteCarlo>
- Lunt, D. J., Foster, G. L., Haywood, A. M., & Stone, E. J. (2008). Late Pliocene Greenland glaciation controlled by a decline in atmospheric CO₂ levels. *Nature*, 454(7208), 1102–1105. <https://doi.org/10.1038/nature07223>
- Lunt, D. J., Haywood, A. M., Schmidt, G. A., Salzmann, U., Valdes, P. J., & Dowsett, H. J. (2010). Earth system sensitivity inferred from Pliocene modelling and data. *Nature Geoscience*, 3(1), 60–64. <https://doi.org/10.1038/ngeo706>
- Martin, C. L., & Tortell, P. D. (2006). Bicarbonate transport and extracellular carbonic anhydrase activity in Bering Sea phytoplankton assemblages: Results from isotope disequilibrium experiments. *Limnology and Oceanography*, 51(5), 2111–2121. <https://doi.org/10.4319/lo.2006.51.5.2111>
- Martin, C. L., & Tortell, P. D. (2008). Bicarbonate transport and extracellular carbonic anhydrase in marine diatoms. *Physiologia Plantarum*, 133(1), 106–116. <https://doi.org/10.1111/j.1399-3054.2008.01054.x>

- Martinez-Boti, M. A., Foster, G. L., Chalk, T. B., Rohling, E. J., Sexton, P. F., Lunt, D. J., et al. (2015). Plio-Pleistocene climate sensitivity evaluated using high-resolution CO₂ records. *Nature*, 518(7537), 49–54. <https://doi.org/10.1038/nature14145>
- Martínez-García, A., Rosell-Melé, A., Jaccard, S. L., Geibert, W., Sigman, D. M., & Haug, G. H. (2011). Southern Ocean dust–climate coupling over the past four million years. *Nature*, 476(7360), 312–315. <https://doi.org/10.1038/nature10310>
- Maslin, M. A., Haug, G. H., Sarnthein, M., & Tiedemann, R. (1996). The progressive intensification of northern hemisphere glaciation as seen from the North Pacific. *Geologische Rundschau*, 85(3), 452–465. <https://doi.org/10.1007/BF02369002>
- Maslin, M. A., Li, X.-S., Loutre, M.-F., & Berger, A. (1998). The contribution of orbital forcing to the progressive intensification of Northern Hemisphere glaciation. *Quaternary Science Reviews*, 17(4-5), 411–426. [https://doi.org/10.1016/S0277-3791\(97\)00047-4](https://doi.org/10.1016/S0277-3791(97)00047-4)
- Matthiessen, J., Knies, J., Vogt, C., & Stein, R. (2009). Pliocene palaeoceanography of the Arctic Ocean and subarctic seas. *Philosophical Transactions of the Royal Society A: Mathematical, Physical and Engineering Sciences*, 367(1886), 21–48. <https://doi.org/10.1098/rsta.2008.0203>
- McKay, R., Naish, T., Carter, L., Riesselman, C., Dunbar, R., Sjunneskog, C., et al. (2012). Antarctic and Southern Ocean influences on Late Pliocene global cooling. *Proceedings of the National Academy of Sciences of the United States of America*, 109(17), 6423–6428. <https://doi.org/10.1073/pnas.1112248109>
- Mejia, L. M., Méndez-Vicente, A., Abrevaya, L., Lawrence, K. T., Ladlow, C., Bolton, C., et al. (2017). A diatom record of CO₂ decline since the late Miocene. *Earth and Planetary Science Letters*, 479, 18–33. <https://doi.org/10.1016/j.epsl.2017.08.034>
- Montañez, I. P., McElwain, J. C., Poulsen, C. J., White, J. D., DiMichele, W. A., Wilson, J. P., et al. (2016). Climate, pCO₂ and terrestrial carbon cycle linkages during late Palaeozoic glacial-interglacial cycles. *Nature Geoscience*, 9(11), 824–828. <https://doi.org/10.1038/ngeo2822>
- Mook, W. G., Bommerso, J. C., & Staverma, W. H. (1974). Carbon isotope fractionation between dissolved bicarbonate and gaseous carbon-dioxide. *Earth and Planetary Science Letters*, 22(2), 169–176. [https://doi.org/10.1016/0012-821X\(74\)90078-8](https://doi.org/10.1016/0012-821X(74)90078-8)
- Mudelsee, M., & Raymo, M. E. (2005). Slow dynamics of the Northern Hemisphere glaciation. *Paleoceanography*, 20, PA4022. <https://doi.org/10.1029/2005PA001153>
- Naish, T., Powell, R., Levy, R., Wilson, G., Scherer, R., Talarico, F., et al. (2009). Obliquity-paced Pliocene West Antarctic ice sheet oscillations. *Nature*, 458(7236), 322–328. <https://doi.org/10.1038/nature07867>
- Onodera, J., Takahashi, K., & Honda, M. C. (2005). Pelagic and coastal diatom fluxes and the environmental changes in the northwestern North Pacific during December 1997–May 2000. *Deep Sea Research, Part II*, 52(16-18), 2218–2239. <https://doi.org/10.1016/j.dsr2.2005.07.005>
- Pagani, M. (2002). The alkenone-CO₂ proxy and ancient atmospheric carbon dioxide. *Philosophical Transactions of the Royal Society A: Mathematical, Physical and Engineering Sciences*, 360(1793), 609–632. <https://doi.org/10.1098/rsta.2001.0959>
- Pagani, M., Liu, Z., LaRiviere, J., & Ravelo, A. C. (2010). High Earth-system climate sensitivity determined from Pliocene carbon dioxide concentrations. *Nature Geoscience*, 3(1), 27–30. <https://doi.org/10.1038/ngeo724>
- Pagani, M., Zachos, J. C., Freeman, K. H., Tipler, B., & Bohaty, S. (2005). Marked decline in atmospheric carbon dioxide concentrations during the Paleogene. *Science*, 309(5734), 600–603. <https://doi.org/10.1126/science.1110063>
- Popp, B. N., Laws, E. A., Bidigare, R. R., Dore, J. E., Hanson, K. L., & Wakeham, S. G. (1998). Effect of phytoplankton cell geometry on carbon isotopic fractionation. *Geochimica et Cosmochimica Acta*, 62(1), 69–77. [https://doi.org/10.1016/S0016-7037\(97\)00333-5](https://doi.org/10.1016/S0016-7037(97)00333-5)
- R Core Team (2017). *R: A language and environment for statistical computing*. Vienna, Austria: R Foundation for Statistical Computing. Retrieved from <https://www.R-project.org/>
- Rau, G. H., Chavez, F. P., & Friederich, G. E. (2001). Plankton ¹³C/¹²C variations in Monterey Bay, California: Evidence of non-diffusive inorganic carbon uptake by phytoplankton in an upwelling environment. *Deep Sea Research, Part I*, 48(1), 79–94. [https://doi.org/10.1016/S0967-0637\(00\)00039-X](https://doi.org/10.1016/S0967-0637(00)00039-X)
- Rau, G. H., Riebesell, U., & Wolf-Gladrow, D. (1996). A model of photosynthetic ¹³C fractionation by marine phytoplankton based on diffusive molecular CO₂ uptake. *Marine Ecology Progress Series*, 133, 275–285. <https://doi.org/10.3354/meps133275>
- Rau, G. H., Riebesell, U., & Wolf-Gladrow, D. (1997). CO_{2(aq)}-dependent photosynthetic ¹³C fractionation in the ocean: A model versus measurements. *Global Biogeochemical Cycles*, 11(2), 267–278. <https://doi.org/10.1029/97GB00328>
- Ravelo, A. C., Andreasen, D. H., Lyle, M., Lyle, A. O., & Wara, M. W. (2004). Regional climate shifts caused by gradual global cooling in the Pliocene epoch. *Nature*, 429(6989), 263–267. <https://doi.org/10.1038/nature02567>
- Raven, J., Giordano, M., Beardall, J., & Maberly, S. C. (2011). Algal and aquatic plant carbon concentrating mechanisms in relation to environmental change. *Photosynthesis Research*, 109(1-3), 281–296. <https://doi.org/10.1007/s11120-011-9632-6>
- Raymo, M. E. (1994). The initiation of Northern Hemisphere glaciation. *Annual Review of Earth and Planetary Sciences*, 22(1), 353–383. <https://doi.org/10.1146/annurev.ea.22.050194.002033>
- Reinfelder, J. R., Kraepiel, A. M. L., & Morel, F. M. M. (2000). Unicellular C₄ photosynthesis in a marine diatom. *Nature*, 407(6807), 996–999. <https://doi.org/10.1038/35039612>
- Reinfelder, J. R., Milligan, A. J., & Morel, F. M. M. (2004). The role of the C₄ pathway in carbon accumulation and fixation in a marine diatom. *Plant Physiology*, 135(4), 2106–2111. <https://doi.org/10.1104/pp.104.041319>
- Reynolds, B. C., Frank, M., & Halliday, A. N. (2008). Evidence for a major change in silicon cycling in the subarctic North Pacific at 2.73 Ma. *Paleoceanography*, 23, PA4219. <https://doi.org/10.1029/2007PA001563>
- Roberts, K., Granum, E., Leegood, R. C., & Raven, J. A. (2007). C₃ and C₄ pathways of photosynthetic carbon assimilation in marine diatoms are under genetic, not environmental, control. *Plant Physiology*, 145(1), 230–235. <https://doi.org/10.1104/pp.107.102616>
- Romanek, C. S., Grossman, E. L., & Morse, J. W. (1992). Carbon isotopic fractionation in synthetic aragonite and calcite: Effects of temperature and precipitation rate. *Geochimica et Cosmochimica Acta*, 56(1), 419–430. [https://doi.org/10.1016/0016-7037\(92\)90142-6](https://doi.org/10.1016/0016-7037(92)90142-6)
- Rosenthal, Y., Dahan, M., & Shemesh, A. (2000). Southern Ocean contributions to glacial-interglacial changes of atmospheric pCO₂: An assessment of carbon isotope record in diatoms. *Paleoceanography*, 15(1), 65–75. <https://doi.org/10.1029/1999PA000369>
- Ruddiman, W. F., & Kutzbach, J. E. (1989). Forcing of late Cenozoic northern hemisphere climate by plateau uplift in southern Asia and the American west. *Journal of Geophysical Research*, 94(D15), 18,409–18,427. <https://doi.org/10.1029/JD094iD15p18409>
- Sarnthein, M., Bartoli, G., Prange, M., Schmittner, A., Schneider, B., Weinelt, M., et al. (2009). Mid-Pliocene shifts in ocean overturning circulation and the onset of quaternary-style climates. *Climate of the Past*, 5(2), 269–283. <https://doi.org/10.5194/cp-5-269-2009>
- Scott, K. M., Henn-Sax, M., Harmer, T. L., Longo, D. L., Frame, C. H., & Cavanaugh, C. M. (2007). Kinetic isotope effect and biochemical characterization of form IA RubisCO from the marine cyanobacterium *Prochlorococcus marinus* MIT9313. *Limnology and Oceanography*, 52(5), 2199–2204. <https://doi.org/10.4319/lo.2007.52.5.2199>
- Seki, O., Foster, G. L., Schmidt, D. N., Mackensen, A., Kawamura, K., & Pancost, R. D. (2010). Alkenone and boron-based Pliocene pCO₂ records. *Earth and Planetary Science Letters*, 292(1-2), 201–211. <https://doi.org/10.1016/j.epsl.2010.01.037>
- Shimada, C., Sato, T., Yamasaki, M., Hasegawa, S., & Tanaka, T. (2009). Drastic change in the late Pliocene subarctic Pacific diatom community associated with the onset of the Northern Hemisphere glaciation. *Paleogeography, Palaeoclimatology, Palaeoecology*, 279(3-4), 207–215. <https://doi.org/10.1016/j.palaeo.2009.05.015>

- Sigman, D. M., Hain, M. P., & Haug, G. H. (2010). The polar ocean and glacial cycles in atmospheric CO₂ concentration. *Nature*, 466(7302), 47–55. <https://doi.org/10.1038/nature09149>
- Sigman, D. M., Jaccard, S. L., & Haug, G. H. (2004). Polar ocean stratification in a cold climate. *Nature*, 428(6978), 59–63. <https://doi.org/10.1038/nature02357>
- Spero, H. J., & Lea, D. W. (1996). Experimental determination of stable isotope variability in Globigerina bulloides: Implications for paleoceanographic reconstructions. *Marine Micropaleontology*, 28(3–4), 231–246. [https://doi.org/10.1016/0377-8398\(96\)00003-5](https://doi.org/10.1016/0377-8398(96)00003-5)
- Stap, L. B., de Boer, B., Ziegler, M., Bintanja, R., Lourens, L. J., & van de Wal, R. S. W. (2016). CO₂ over the past 5 million years: Continuous simulation and new $\delta^{11}\text{B}$ -based proxy data. *Earth and Planetary Science Letters*, 439, 1–10. <https://doi.org/10.1016/j.epsl.2016.01.022>
- Stoll, H. M., Mendez-Vicente, A., Abrevaya, L., Anderson, R. F., Rigual-Hernández, A. S., & Gonzalez-Lemos, S. (2017). Growth rate and size effect on carbon isotopic fractionation in diatom-bound organic matter in recent Southern Ocean sediments. *Earth and Planetary Science Letters*, 457, 87–99. <https://doi.org/10.1016/j.epsl.2016.09.028>
- Studer, A. S., Martínez-García, A., Jaccard, S. L., Girault, F. E., Sigman, D. M., & Haug, G. H. (2012). Enhanced stratification and seasonality in the subarctic Pacific upon Northern Hemisphere glaciation—New evidence from diatom-bound nitrogen isotopes, alkenones and archaeal tetraethers. *Earth and Planetary Science Letters*, 351–352, 84–94. <https://doi.org/10.1016/j.epsl.2012.07.029>
- Sültemeyer, D., Schmidt, C., & Fock, H. P. (1993). Carbonic anhydrases in higher plants and aquatic microorganisms. *Physiologia Plantarum*, 88(1), 179–190. <https://doi.org/10.1111/j.1399-3054.1993.tb01776.x>
- Sumper, M., & Kröger, N. (2004). Silica formation in diatoms: The function of long-chain polyamines and silaffins. *Journal of Materials Chemistry*, 14(14), 2059–2065. <https://doi.org/10.1039/B401028K>
- Swann, G. E. A. (2010). Salinity changes in the North West Pacific Ocean during the late Pliocene/early Quaternary from 2.73 Ma to 2.53 Ma. *Earth and Planetary Science Letters*, 297(1–2), 332–338. <https://doi.org/10.1016/j.epsl.2010.06.035>
- Swann, G. E. A., Maslin, M. A., Leng, M. J., Sloane, H. J., & Haug, G. H. (2006). Diatom $\delta^{18}\text{O}$ evidence for the development of the modern halocline system in the subarctic northwest Pacific at the onset of major Northern Hemisphere glaciation. *Paleoceanography*, 21, PA1009. <https://doi.org/10.1029/2005PA001147>
- Swann, G. E. A., Snelling, A. M., & Pike, J. (2016). Biogeochemical cycling in the Bering Sea over the onset of major Northern Hemisphere glaciation. *Paleoceanography*, 31, 1261–1269. <https://doi.org/10.1002/2016PA002978>
- Swift, D. M., & Wheeler, A. P. (1992). Evidence of an organic matrix from diatom biosilica. *Journal of Phycology*, 28(2), 202–209. <https://doi.org/10.1111/j.0022-3646.1992.00202.x>
- Tabata, S. (1975). The general circulation of the Pacific Ocean and a brief account of the oceanographic structure of the North Pacific Ocean. Part I—Circulation and volume transport. *Atmosphere*, 13, 133–168. <https://doi.org/10.1080/00046973.1975.9648394>
- Takahashi, K. (1986). Seasonal fluxes of pelagic diatoms in the subarctic Pacific, 1982–1983. *Deep Sea Research Part A. Oceanographic Research Papers*, 33(9), 1225–1251. [https://doi.org/10.1016/0198-0149\(86\)90022-1](https://doi.org/10.1016/0198-0149(86)90022-1)
- Takahashi, K., Hisamichi, K., Yanada, M., & Maita, Y. (1996). Seasonal changes of marine phytoplankton productivity: A sediment trap study (in Japanese). *Kaiyo Monthly*, 10, 109–115.
- Takahashi, T., Sutherland, S. C., & Kozyr, A. (2016). Global ocean surface water partial pressure of CO₂ database: Measurements performed during 1957–2015 (2015). ORNL/CDIAC-160, NDP-088(V2015). Carbon Dioxide Information Analysis Center, Oak Ridge National Laboratory, U.S. Department of Energy, Oak Ridge, Tennessee. [https://doi.org/10.3334/CDIAC/OTG.NDP088\(V2015\)](https://doi.org/10.3334/CDIAC/OTG.NDP088(V2015))
- Takahashi, T., Sutherland, S. C., Wanninkhof, R., Sweeney, C., Feely, R. A., Chipman, D. W., et al. (2009). Climatological mean and decadal changes in surface ocean pCO₂, and net sea-air CO₂ flux over the global oceans. *Deep Sea Research Part II*, 56(8–10), 554–577. <https://doi.org/10.1016/j.dsr2.2008.12.009>
- Tiedemann, R., & Haug, G. H. (1995). Astronomical calibration of cycle stratigraphy for Site 882 in the northwest Pacific. In D. K. Rea, I. A. Basov, D. W. Scholl, & J. F. Allan (Eds.), *Proceedings of the Ocean Drilling Program, Scientific Results Volume* (pp. 283–292). College Station, TX: Ocean Drilling Program.
- Tortell, P. D., Martin, C. L., & Corkum, M. E. (2006). Inorganic carbon uptake and intracellular assimilation by subarctic Pacific phytoplankton assemblages. *Limnology and Oceanography*, 51(5), 2102–2110. <https://doi.org/10.4319/lo.2006.51.5.2102>
- Tortell, P. D., & Morel, F. M. M. (2002). Sources of inorganic carbon for phytoplankton in the eastern subtropical and equatorial Pacific Ocean. *Limnology and Oceanography*, 47(4), 1012–1022. <https://doi.org/10.4319/lo.2002.47.4.1012>
- Tortell, P. D., Payne, C., Gueguen, C., Strzepek, R. F., Boyd, P. W., & Rost, B. (2008). Inorganic carbon uptake by Southern Ocean phytoplankton. *Limnology and Oceanography*, 45, 1485–1500.
- Tortell, P. D., Reinfelder, J. R., & Morel, F. M. M. (1997). Active uptake of bicarbonate by diatoms. *Nature*, 390(6657), 243–244. <https://doi.org/10.1038/36765>
- Tortell, P. D., Trimborn, S., Li, Y., Rost, B., & Payne, C. D. (2010). Inorganic carbon utilization by Ross Sea phytoplankton across natural and experimental CO₂ gradients. *Journal of Phycology*, 46(3), 433–443. <https://doi.org/10.1111/j.1529-8817.2010.00839.x>
- Trimborn, S., Lundholm, N., Thoms, S., Richter, K.-U., Krock, B., Hansen, P. J., & Rost, B. (2008). Inorganic carbon acquisition in potentially toxic and non-toxic diatoms: The effect of pH-induced changes in seawater carbonate chemistry. *Physiologia Plantarum*, 133(1), 92–105. <https://doi.org/10.1111/j.1399-3054.2007.01038.x>
- van de Wal, R. S. W., de Boer, B., Lourens, L. J., Köhler, P., & Bintanja, R. (2011). Reconstruction of a continuous high-resolution CO₂ record over the past 20 million years. *Climate of the Past*, 7, 1459–1469.
- Waddell, L. M., Hendy, I. L., Moore, T. C., & Lyle, M. W. (2009). Ventilation of the abyssal Southern Ocean during the late Neogene: A new perspective from the subantarctic Pacific. *Paleoceanography*, 24, PA3206. <https://doi.org/10.1029/2008PA001661>
- Weiss, R. F. (1970). The solubility of nitrogen, oxygen and argon in water and seawater. *Deep Sea Research*, 17, 721–735.
- Weiss, R. F. (1974). Carbon dioxide in water and seawater: The solubility of a non-ideal gas. *Marine Chemistry*, 2(3), 203–215. [https://doi.org/10.1016/0304-4203\(74\)90015-2](https://doi.org/10.1016/0304-4203(74)90015-2)
- Willeit, M., Ganopolski, A., Calov, R., Robinson, A., & Maslin, M. (2015). The role of CO₂ decline for the onset of northern hemisphere glaciation. *Quaternary Science Reviews*, 119, 22–34. <https://doi.org/10.1016/j.quascirev.2015.04.015>
- Yu, J., Elderfield, H., & Hönisch, B. (2007). B/Ca in planktonic foraminifera as a proxy for surface seawater pH. *Paleoceanography*, 22, PA2202. <https://doi.org/10.1029/2006PA001347>